REVISTA FLORESTA Engenharia Florestal
ISSN 1982-4688
Edição 55
Universidade Federal do Paraná
Setor de Ciências Agrárias

RELATIONSHIPS BETWEEN LANDSAT 8 OLI PRODUCTS, MOISTURE, AND SURFACE FUEL LOAD IN CERRADO GRASSLAND ENVIRONMENTS

Micael Moreira Santos, Antônio Carlos Batista, Olavo da Costa Leite, Jader Nunes Cachoeira, Gil Rodrigues Dos Santos, Marcos Giongo

[1*] Universidade Federal do Paraná – Curitiba, Paraná, Brasil - micaelmoreira@ufpr.br
[2] Universidade Federal do Paraná – Curitiba, Paraná, Brasil - batistaufpr@gmail.com
[3] Instituto Federal do Tocantins – Palmas, Tocantis, Brasil - olavol@hotmail.com
[4]Universidade Federal do Tocantins – Palmas, Tocantins, Brasil - jadernunes@uft.edu.br
[5]Universidade Federal do Tocantins – Palmas, Tocantins, Brasil - giongo@uft.edu.br

Received for publication: 12/11/2024 – Accepted for publication: 21/03/2025

Resumo

Relações entre produtos de Landsat 8 OLI e umidade e carga de material combustível superficial em ambiente campestre de Cerrado. Este estudo teve como objetivo avaliar as relações entre os produtos do Landsat 8 OLI e a carga e umidade do combustível superficial em ambientes campestres do Cerrado. Foram coletadas 68 unidades de amostragem, mantendo um distanciamento mínimo de 100 metros entre elas. Os valores dos *pixels* associados às parcelas de campo foram obtidos a partir de uma janela de 3 x 3 *pixels*, extraindo-se os valores medianos de cada polígono. Após obter as imagens de satélite correspondentes ao período de coleta dos dados *in loco* e tabular as informações, realizou-se análises de correlação linear de Pearson entre a carga do combustível e as variáveis independentes derivadas do processamento das imagens. As correlações mais significativas ocorreram entre combustível herbáceo morto e fração-solo das análises de mistura espectral, com r = -0,81 para carga e r = -0,60 para umidade. Em relação à reflectância das bandas do Landsat 8, as maiores correlações foram entre combustível herbáceo morto e o infravermelho próximo, com r = -0,68 (carga) e r = -0,61 (umidade). Nos índices de vegetação, destacaram-se as correlações entre combustível herbáceo morto e os índices MSI (r = 0,77), NDII6 e GVMI (r = -0,77) para carga de combustível. Para a umidade do combustível, houve correlações negativas com os índices DER23 (r = -0,57) e MNDWI (r = -0,56) e positiva com o MSI (r = 0,47). As relações foram mais fortes entre carga e umidade nas classes de combustíveis mortos, especialmente com a carga de combustível herbáceo morto.
Palavras-chave: carga do combustível; umidade; correlações lineares; imagens de satélite; processamento de imagens.

Abstract

This study evaluated the relationships among Landsat 8 OLI products, surface fuel load, and moisture content in Cerrado grassland environments. Sixty-eight sampling units, with a minimum distance of 100 m between them, were used in this study. The pixel values associated with the field plots were obtained from a 3 x 3-pixel window by extracting the median values of each polygon. After receiving the satellite images corresponding to the *in situ* data collection period and tabulating the information, Pearson's linear correlation analyses were performed between the fuel load and independent variables derived from image processing. Dead herbaceous fuel and the soil fraction of the spectral mixture analyses showed strong correlations, with r = -0.81 for load and r = -0.60 for moisture content. For reflectance of the Landsat 8 bands, the highest correlations were observed between dead herbaceous fuel and near-infrared, with r = -0.68 (load) and r = -0.61 (moisture). The correlations between dead herbaceous fuel and the MSI (r = 0.77), NDII6, and GVMI (r = -0.77) indices for fuel load stood out among the vegetation indices. Fuel moisture was negatively correlated with the DER23 (r = -0.57) and MNDWI (r = -0.56) indices and positively correlated with MSI (r = 0.47). The relationships between load and moisture in the dead fuel classes were more substantial, particularly for the dead herbaceous fuel load.
Keywords: fuel load; moisture; linear correlations; satellite images; image processing.

INTRODUCTION

Forest fires can cause serious damage to forests and neighboring communities because they can spread rapidly over large areas and act as a disturbance factor of considerable importance in ecosystems, leading to drastic changes in the structure and function of vegetation (LECINA-DIAZ *et al.*, 2021). In the context of forest fires, fuel is one of the main factors that are considered for fire management and the only factor that can be controlled through human action (ROTHERMEL, 1972).

The description and quantification of flammable materials are essential for correctly understanding fire behavior. This information is highly relevant for fire management, the execution of controlled burns, firefighting activities, and forest fire risk assessment. In addition, these data allow the creation of models for quantification of

carbon (KENNEDY *et al.*, 2020). However, determining fuel characteristics through field investigation is highly complex and requires considerable operational time and field campaigns to achieve representative sample sizes for a given population (FORBES *et al.*, 2022). Thus, indirect methods such as biophysical modeling can be used to estimate parameters that are difficult to obtain directly. Given that fuel is the result of vegetation properties at a specific location, biophysical models can be used to predict quantitative fuel attributes (GALE *et al.*, 2021). However, indirect determination of surface fuel through mathematical modeling in Cerrado environments has rarely been performed and scientifically validated owing to the scarcity of studies conducted in these biomes.

The use of remote sensing techniques for indirect estimation, classification, and determination of surface fuel attributes is crucial for obtaining data remotely with greater agility and lower costs. Remote sensing techniques are essential for estimating various fuel characteristics and are being increasingly investigated and improved. According to Sharma and Dhakal (2021), among different remote sensing techniques, the products obtained can help assess the risk of forest fires, including (i) indirect measurements of live fuel moisture, (ii) measurement of live herbaceous biomass, (iii) fuel condition assessments, and (iv) fuel type classification.

Among the studies conducted using remote-sensing products to determine the relationships between different surface fuel attributes, Franke *et al.* (2018) studied the relationships between products from spectral mixture analysis (SMA) and surface fuel in a Cerrado grassland environment. Some studies used reflectance values from satellite images (e.g., MARINO *et al.*, 2020; HADI *et al.*, 2016; MERRILL *et al.*, 1993; ZHANG *et al.*, 2018) and the calculation of vegetation indices (VIs) and their relationships with biomass characteristics (e.g., DANSON; BOWYER, 2004; GAO *et al.*, 2020; GARCÍA *et al.*, 2020; ZORMPAS *et al.*, 2017). Despite several studies using remote-sensing techniques and products to estimate and map surface fuel characteristics, scientific research on fuels from Cerrado biomes is scarce.

Given the heterogeneity and complexity of obtaining information on fuel in these biomes, it is essential to understand the relationships between the spectral responses from satellite images and characteristics of Cerrado fuel. The present study was based on the following hypotheses: (i) There are relationships among the fraction values obtained by SMA of green vegetation, non-photosynthetic dry vegetation, and soil versus the load and moisture variables of the surface fue; (ii) There are relationships among the reflectance values and VIs versus the load and moisture variables of the surface fuel. Thus, the general objective of this study was to evaluate the relationships between the data from the Landsat 8 OLI sensor and the load as well as moisture of surface fuel during the dry season in a Cerrado grassland environment.

MATERIALS AND METHODS

Study area

Field investigation was conducted at the south-central portion of the Serra Geral do Tocantins Ecological Station (EESGT), a fully protected conservation unit located in the Cerrado biome of the Jalapão region, which has an area of 716,306 ha. The EESGT covers five municipalities namely Almas, Mateiros, Ponte Alta, and Rio da Conceição, which belong to the state of Tocantins, and Formosa do Rio Preto, which belongs to the state of Bahia.

According to the Köppen climate classification, the climate of the region is Aw (tropical savanna climate), with annual precipitation ranging from 1,400 to 1,500 mm, which is higher than the annual potential evapotranspiration. The summer is rainy, occurring between October and April, and the winter is dry, occurring between May and September (ICMBIO, 2014).

In the study region, the predominant phytophysiognomy is grassland with the following types: clear, clear wet, dirty, dirty wet, and rocky fields (RIBEIRO; WALTER, 2008). The predominant soil type is quartz sand or quartzarenic neosol, with a sand or loamy sand texture at a depth of at least two meters and may have up to 15% clay. The relief varies from relatively flat to gently undulating, with average altitude of 300–500 m (ICMBIO, 2014).

Field survey

A field study was conducted to assess the surface fuel load variables by establishing sampling plots. Data were collected during four distinct intervals: (i) May 11 to May 31, 2017; (ii) June 6 to June 29, 2017; (iii) August 5 to August 25, 2017; and (iv) September 8 to September 24, 2017. A field survey of the surface fuel load variables was conducted by installing data sampling units with two transects of 30 m. By marking the transects, eight subsamples, called fuel data sampling units, were installed, employing a previous desing in which a destructive method collected the fuel. These sub-plots had an area of 0.25 m² (0.5 cm × 0.5 cm), enabling exhaustive sampling and providing significant variability of the sampled fuel in a shorter time (Figure 1).

REVISTA FLORESTA
Engenharia Florestal
ISSN 1982-4688
Edição 55
Universidade Federal do Paraná
Setor de Ciências Agrárias

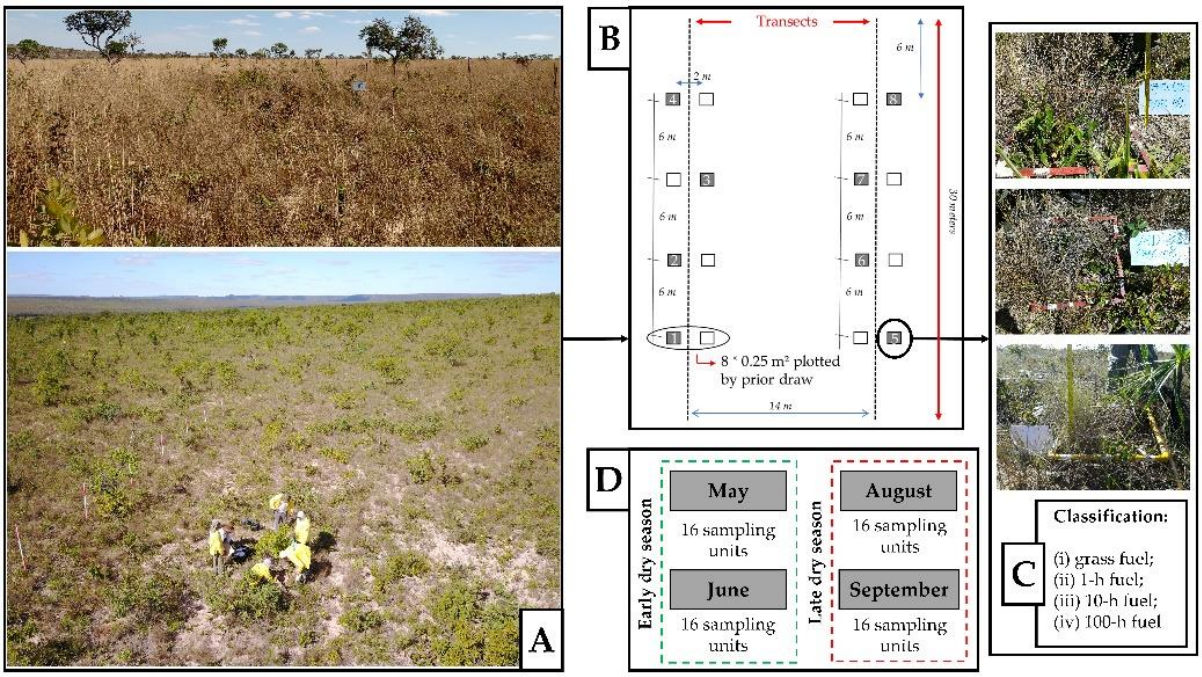

Figure 1. Experimental design used for fuel sampling
Figura 1. Delineamento experimental utilizado nas coletas de material combustível

Thus, 128 data sampling units were used for a totaling of 1,024 fuel data sampling units. However, to estimate the fuel load values using satellite images, 68 data sampling units were chosen considering the location of the sampling units and their respective distances from each other, with distances of greater than 100 m between sampling units .

Destructive sampling was performed by separating the material according to its physiological state (live or dead) among different diameter classes (time lag) according to the methodology proposed by Schroeder and Buck (1970). Thus, live fuels were classified as follows: (i) dead grass fuel, (ii) 1-h downed wood debris (<0.64 cm in diameter), (iii) live grass fuel, and (iv) live shrub fuel (<0.64 cm in diameter). Since the purpose was to assess fine fuels smaller than 0.64 cm in diameter, which play a critical role in fire propagation within open vegetation areas of Cerrado biomes, the larger 10-h (0.64–2.54 cm) and 100-h (2.54–7.62 cm) fuel classes were excluded from consideration. In addition to these classes, the analysis and estimations included the total fine live fuels (grass + shrub < 0.64 cm diameter), total fine dead fuels (grass + 1-h downed wood debris), and total fine fuel load (live and dead; <0.64 cm diameter).

A subsample was separated from each fuel class, packaged in a kraft paper bag, duly identified, and weighed on a digital scale to determine its respective mass before drying. After field collection, all subsamples were subjected to laboratory drying in an oven at 75 °C for 48 h. Subsequently, the dry mass and moisture content of the fuels were determined by the ratio of the difference between the wet mass and dry mass on a dry basis and then transformed into percentages.

Satelite image acquisition and processing

The images used in this study were obtained from the Landsat 8 OLI satellite and were downloaded free of charge from the EarthExplorer platform (earthexplorer.usgs.gov) of the United States Geological Survey (USGS). The images obtained were from dates close to those of field sampling during the four collections carried out during the dry season of the year 2017: May, June, August, and September. It is worth mentioning that the downloaded images were used to perform the SMA.

After obtaining the images, they were subjected to an atmospheric correction process to eliminate atmospheric interference in data extraction and obtain the reflectance values. The Landsat 8 OLI surface reflectance data were generated using the Land Surface Reflectance Code (LaSRC) algorithm (VERMOTE *et al.*, 2018). Reflectance values were obtained from the Landsat 8 OLI sensor bands in the following channels: (i) blue (0.45–0.51 µm), (ii) green (0.53–0.59 µm), (iii) red (0.64–0.67 µm), (iv) near-infrared (0.85–0.88 µm), (v) shortwave infrared (1.57–1.65 µm), and (vi) shortwave infrared (2.11–2.29 µm).

The Google Earth Engine (GEE) cloud-based geospatial data processing platform was used to extract the reflectance values of the bands and calculate the VIs. The GEE platform provides easy access to high-performance computing resources for large-scale processing of geospatial databases (GORELICK *et al.*, 2017). In this manner,

data were extracted from different images and spectral bands, and several VIs were calculated simultaneously, quickly, and without using the physical memory of the computer.

The values of the pixels associated with the field plots were extracted from a 3 x 3-pixel window around the reference pixel associated with the field plot. Thus, the median values were extracted from the pixels of each 3 × 3-pixel polygon linked to the field plots (CHRYSAFIS *et al.*, 2017; CHUVIECO *et al.*, 2002). The data were exported and tabulated to associate the information from the plots collected in the field with thatat from SMA, reflectance, and calculated VIs.

Calculation of VIs

VIs were calculated by combining the reflectance values of different spectral bands. VIs are an efficient means of obtaining empirical information from multispectral sensors and are commonly used in scientific studies to better explain or determine the behavior of certain vegetation variables (e.g., YEBRA *et al.*, 2018).

Therefore, a total of 20 VIs were calculated and incorporated into the analyses as independent variables: (i) Normalized Difference Vegetation Index (NDVI), (ii) Visible Atmospherically Resistant Index (VARI), (iii) Visible Green Index (VIgreen), (iv) Simple Ratio (SR), (v) Structure Insensitive Pigment Index (SIPI), (vi) Soil-Adjusted Vegetation Index (SAVI), (vii) Normalized Difference Water Index (NDWI), (viii) Normalized Difference Infrared Index (NDII6), (ix) Normalized Burn Ratio (NBR), (x) Modified Vegetation Index (MVI), (xi) Modified Simple Ratio (MSR), (xii) Moisture Stress Index (MSI), (xiii) Modified Normalized Difference Water Index (MNDWI), (xiv) Integral (INT), (xv) Global Vegetation Moisture Index (GVMI), (xvi) Enhanced Vegetation Index (EVI), (xvii) Derivative-band 5 (ivp), band 6 (siwir1) (DER56), (xviii) Derivative-band 4 (vm), band 5 (ivp) (DER45), (xix) Derivative-band 3 (vd), band 4 (vm) (DER34), and (xx) Derivative-band 2 (az), band 3 (vd) (DER23). The VIs analyzed in this study showed relationships with fuel load and moisture as well as the physiological state of the fuel. These VIs were chosen to analyze their viability for estimating the fuel load from Landsat 8 OLI images, considering seasonality during the dry season in a Cerrado environment.

Spectral mixture analysis

A spectral library was constructed after processing the satellite images. To achieve this, the surface targets of SMA were first divided into (i) non-photosynthetic dry vegetation (NPV), (ii) green vegetation (GV), and (iii) exposed soil (soil fraction, SF). Figure 2 presents a summary of the data processing from remote sensing.

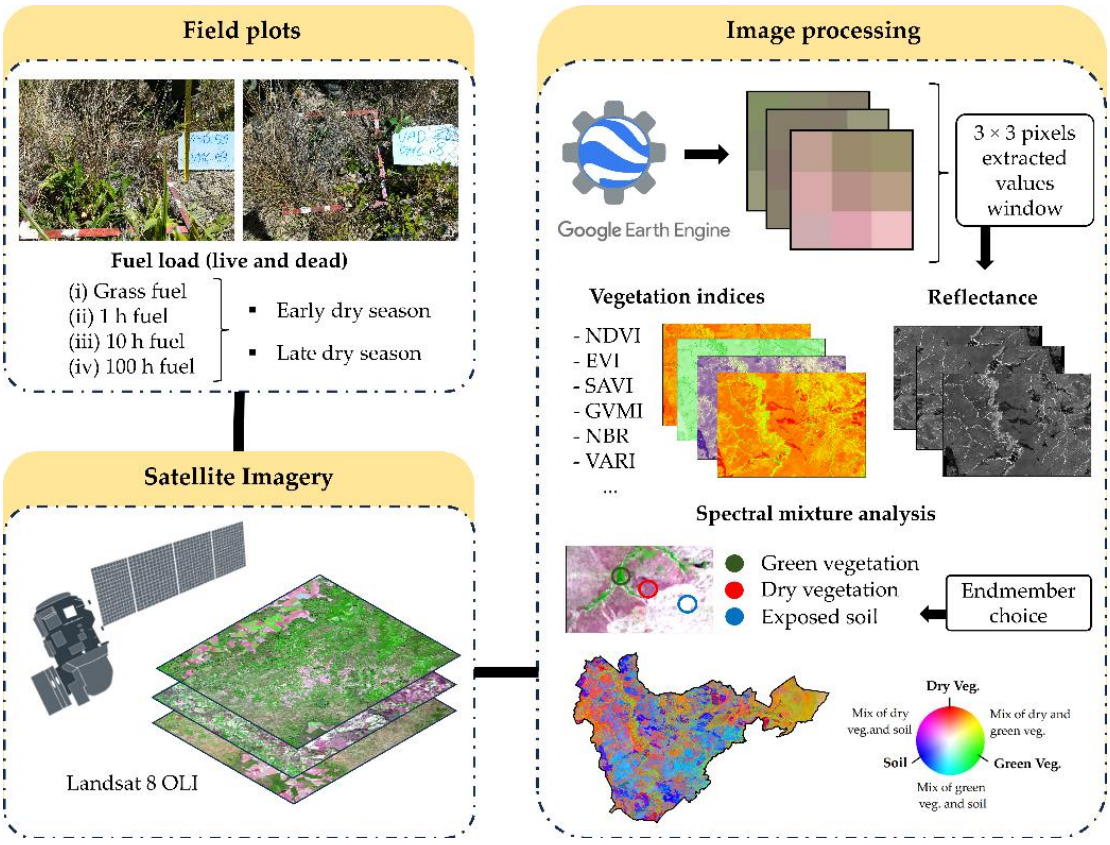

Figure 2. Summary of data processing from remote sensing
Figura 2. Síntese do processamento dos dados provenientes do sensoriamento remoto

Thus, several candidates for "pure pixels" called endmembers were selected from each target. Using the distinct reflectance patterns of each target, regions of interest (ROI) were defined to ensure that their reflectance closely matched the characteristic curve of the respective target.

To achieve the objectives proposed here, endmembers were chosen in four representative images of the four months of the dry season covered in this study (May, June, August and September), with the dates: 05/05/2017, 06/06/2017, 06/22/2017, 07/24/2017, 08/09/2017, and 09/10/2017. Thus, with all candidates for pure pixels of the desired features chosen based on the spectral curves, the selection of endmembers based on their statistical metrics began with specific software. This procedure is based on multiple endmember spectral mixture analysis (MESMA) methodology.

The lowest Endmember Average RMSE (EAR) and Minimum Average Spectral Angle (MASA) values were used to select the most representative values. This enabled the analysis of various configurations that accounted for the meteorological variations during the dry period.

Statistical analysis

After processing the satellite image data, all the information associated with the field sampling points was extracted. All the extracted data were tabulated and correlated using Pearson's correlation analysis ($p < 0.05$; $p < 0.01$). Data normality was assessed using the Shapiro-Wilk test ($\alpha = 0.05$) prior to conducting Pearson's correlation analysis. All the variables met the normality assumption, supporting the use of parametric statistical methods.

Correlations were performed between fuel load and moisture variables, especially for the 1-h dead fuel classes (dead grass; 1-h downed wood debris; 1-h total dead), 1-h total fuel (live and dead), and remote sensing products, such as fraction values from SMA, reflectance values from satellite images, and calculated VIs.

RESULTS

Fuel load and moisture

The fuel load values obtained through field sampling across the entire data collection period (May, June, August, and September) ranged from 0.19 to 1.97 Mg ha^{-1} for live grass fuel (coefficient of variation, CV = 7.0%), with an average of 0.91 Mg ha^{-1}. Meanwhile, for live shrub fuel (CV = 26.2%), the values ranged from 0.3 to 3.9 Mg ha^{-1} with an average of 1.54 Mg ha^{-1}. For dead grass fuel (CV = 7.6%), the load quantities varied from 0.0 to 2.8 Mg ha^{-1}, presenting an average of 1.18 Mg ha^{-1}. Furthermore, 1-h downed wood debris (CV = 27.1%) varied from 0.17 to 4.1 Mg ha^{-1} with an average value of 1.59 Mg ha^{-1}.

Regarding the moisture values of the fuel in the different classes, it was observed that for live grass fuel the moisture content showed an average of 60.1% and ranged from 34.8% to 85.0%, whereas for the 1-h live woody class the average moisture content was 91.3% with a range of 62.8–123.6%. The total amount of fine live fuel averaged 77.1%, ranging from 54.9% to 100.1%. For dead fuel, the moisture content of the dead grass fuel class presented an average of 9.9%, ranging from 0.4% to 25.4%, whereas 1-h downed wood debris presented an average of 8.0%, ranging from 0.8% to 19.8%.

Correlations between variables

Correlations involving fraction values from SMA

Figure 3 presents the Pearson correlations, highlighting the relationships between the variables obtained from SMA (fractions of NPV, GV, and SF) and the fuel load variables. It can be observed that strong correlations were observed for the dead fuel variables, especially with dead grass fuel load and total fine fuel load (live and dead; <0.64 cm diameter). The strongest correlation observed was between dead grass fuel and 1-h downed wood debris vs. the soil fraction (of the SMA) with $r = -0.81$ and $r = -0.77$, respectively ($p < 0.01$). Therefore, inverse correlations between such variables can be observed as the load of both variables (dead grass and 1-h downed wood debris) increases and the fraction of exposed soil decreases.

Next, the correlation between dead grass fuel and 1-h downed wood debris and the NPV fraction showed $r = 0.75$ and $r = 0.67$, respectively ($p < 0.01$), indicating a direct correlation. Weaker, non-significant correlations ($p > 0.05$) with the fraction values of the SMA were observed for the live fuel classes.

Regarding the relationships between the moisture content of the fuel and the fraction values of the SMA, it can be observed that the strong correlations are related to the dead fuel classes, with the strongest correlations being between the moisture content of dead grass fuel and 1-h downed wood debris vs. the SF, which presented $r = -0.60$ and $r = -0.58$, respectively ($p < 0.01$), as shown in Figure 3. Subsequently, the dead grass fuel moisture class showed significant correlations with the GV and NPV fractions, with $r = -0.58$ and $r = -0.55$ ($p < 0.01$), respectively.

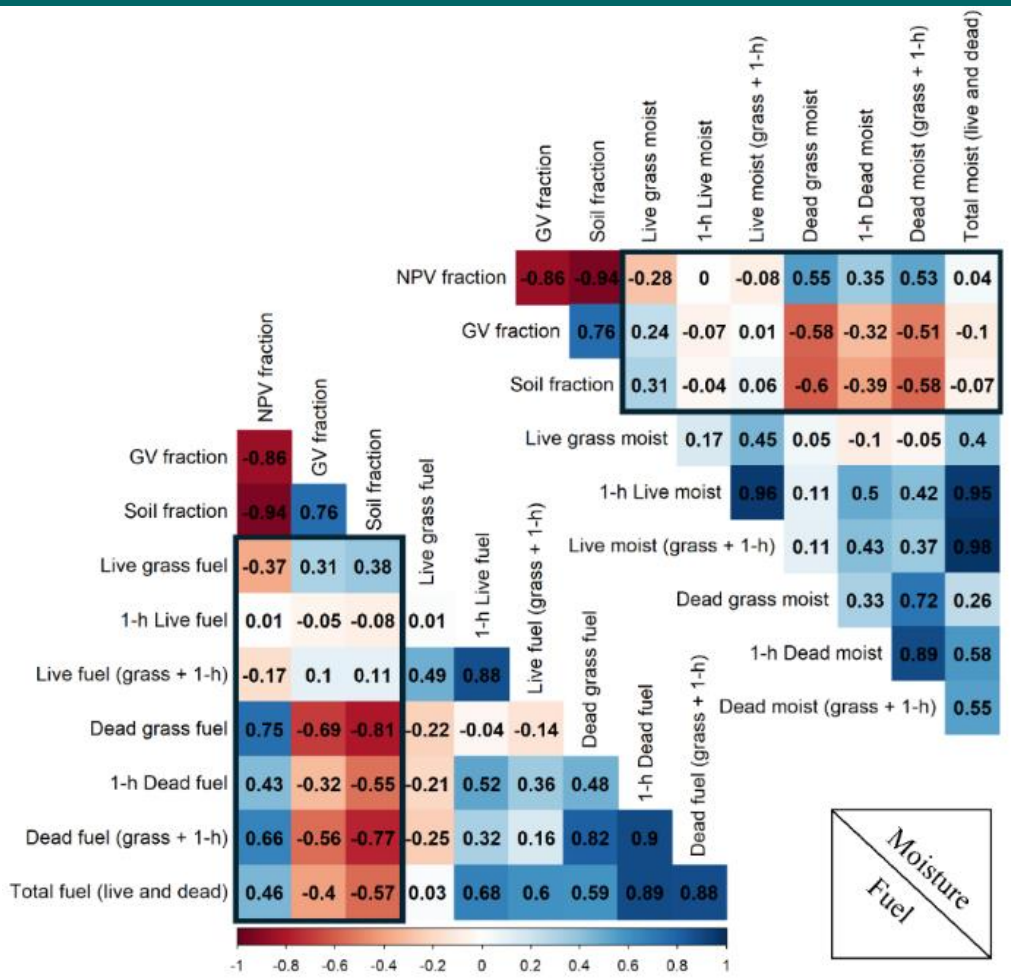

Figure 3. Correlations between moisture content and fuel load for different classes and fraction values from spectral mixture analysis

Figura 3. Correlações entre a umidade e carga de combustível nas diferentes classes e os valores fração da análise de mistura espectral

Weaker and non-significant correlations ($p < 0.01$; $p < 0.05$) were observed between moisture content and the variables from SMA such as live shrub fuel (<0.64 cm in diameter), total fine live fuel (grass + shrub < 0.64 cm diameter), and total fine fuel load (live and dead; <0.64 cm diameter).

Correlations with reflectance values from the Landsat 8 OLI sensor

Figure 4 shows the correlations between the reflectance values of the Landsat 8 OLI satellite bands and fuel load variables. The strongest correlations observed between these variables were the inverse relationships between the reflectance of the near-infrared region (band 5) and the dead grass fuel and total fine dead fuel (dead grass + 1-h downed wood debris), with $r = -0.68$ and $r = -0.60$, respectively ($p < 0.01$). These fuel variables (dead grass and 1-h downed wood debris) also showed a significant inverse correlation with the band that covers the green region of the electromagnetic spectrum, with $r = -0.56$ and $r = -0.52$, respectively. Therefore, more significant reflectance responses to changes in dead fuel loads were observed in the grassland areas of the Cerrado biome. Weak correlations were found for live fuel load as an example of the relationship between fuel variables and SMA fraction values.

Considering the relationships between the moisture content of the fuel in the different classes and the reflectance variables of Landsat 8 OLI images, it can be noted that the moisture content of dead fuel presented the strongest correlations, followed by the variables from SMA. Among them, the correlations between the moisture content of dead grass fuel and near-infrared (NIR) light ($r = -0.61$; $p < 0.01$) and the reflectance of the green region ($r = -0.56$; $p < 0.01$) stand out. The moisture content of live grass fuel and its correlation with the reflectance variables were among the weakest correlations and were not statistically significant (Figure 4).

REVISTA FLORESTA Engenharia Florestal
ISSN 1982-4688
Edição 55
Universidade Federal do Paraná
Setor de Ciências Agrárias

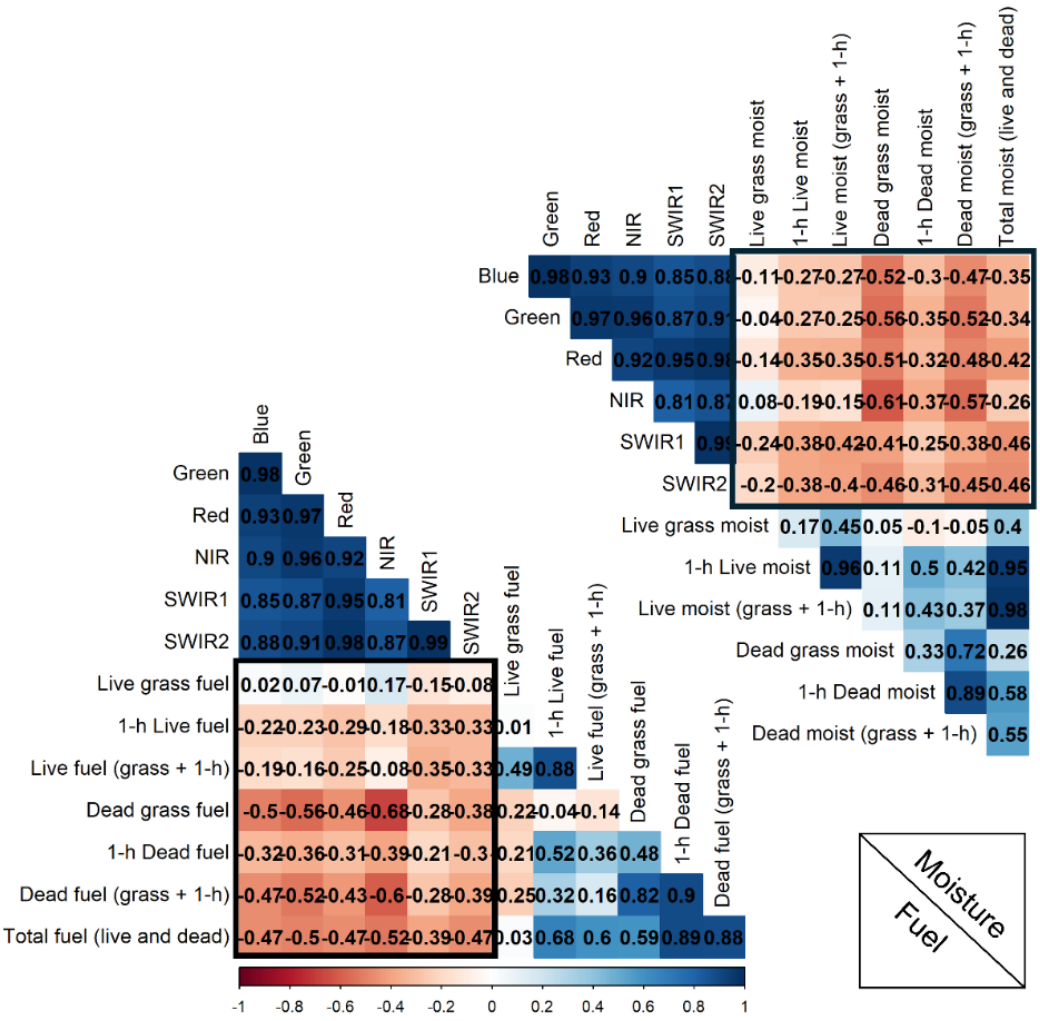

Figure 4. Correlations between moisture content and fuel load for different classes and reflectance values of satellite images

Figura 4. Correlações entre a umidade e carga de combustível nas diferentes classes e os valores de reflectância das imagens de satélite

Correlations with VIs

Among the correlations between the fuel load variables and VIs tested in this study, NDII6, MSI, and GVMI stood out. Figure 5 shows the correlations between fuel load variables and the calculated VIs. As in previous examples, dead grass fuel load presented more excellent inverse correlations with the NDII6 and GVMI indices ($r = -0.77$) and a direct correlation with the MSI index ($r = 0.77$; $p < 0.01$).

Analyzing the relationships regarding the total amount of live and dead fuel with a diameter of less than 0.7 cm (Tot07), it was observed that only the VIs VARI and VI did not present significant correlations between themselves, with values of $r = 0.17$ and $r = 0.18$, respectively ($p > 0.05$). These VIs presented significant relationships only with live fuel variables; only VARI and VI showed significant relationships with all live fuel variables studied here. However, VIs also showed significant relationships only with dead fuel variables, as was the case for the MNDWI and DER23 indices ($p < 0.01$). Apart from VARI, VI, MNDWI, and DER23 indices, which showed more specific interactions with the live (VARI and VI) or dead (MNDWI and DER23) fuel classes, the other VIs showed significant interactions with at least one live fuel variable and one dead fuel variable.

Regarding the moisture content of the fuel and its correlations with the calculated VIs, significant linear relationships were observed between the fuel moisture variables and the SR, NDVI, SAVI, MVI, and MSR indices (Figure 5). These VIs presented strong relationships with the total fine fuel load (live and dead; <0.64 cm diameter) moisture content, with positive correlations of $r = 0.58$ for SR and $r = 0.57$ for NDVI, SAVI, MVI, and MSR ($p < 0.01$). Also noteworthy were the VIs DER23 and MNDWI, which showed the best inverse correlations ($r = -0.57$ and $r = 0.56$, respectively) with the moisture content of dead grass fuel ($p < 0.01$).

REVISTA FLORESTA
Engenharia Florestal
ISSN 1982-4688
Edição 55
Universidade Federal do Paraná
Setor de Ciências Agrárias

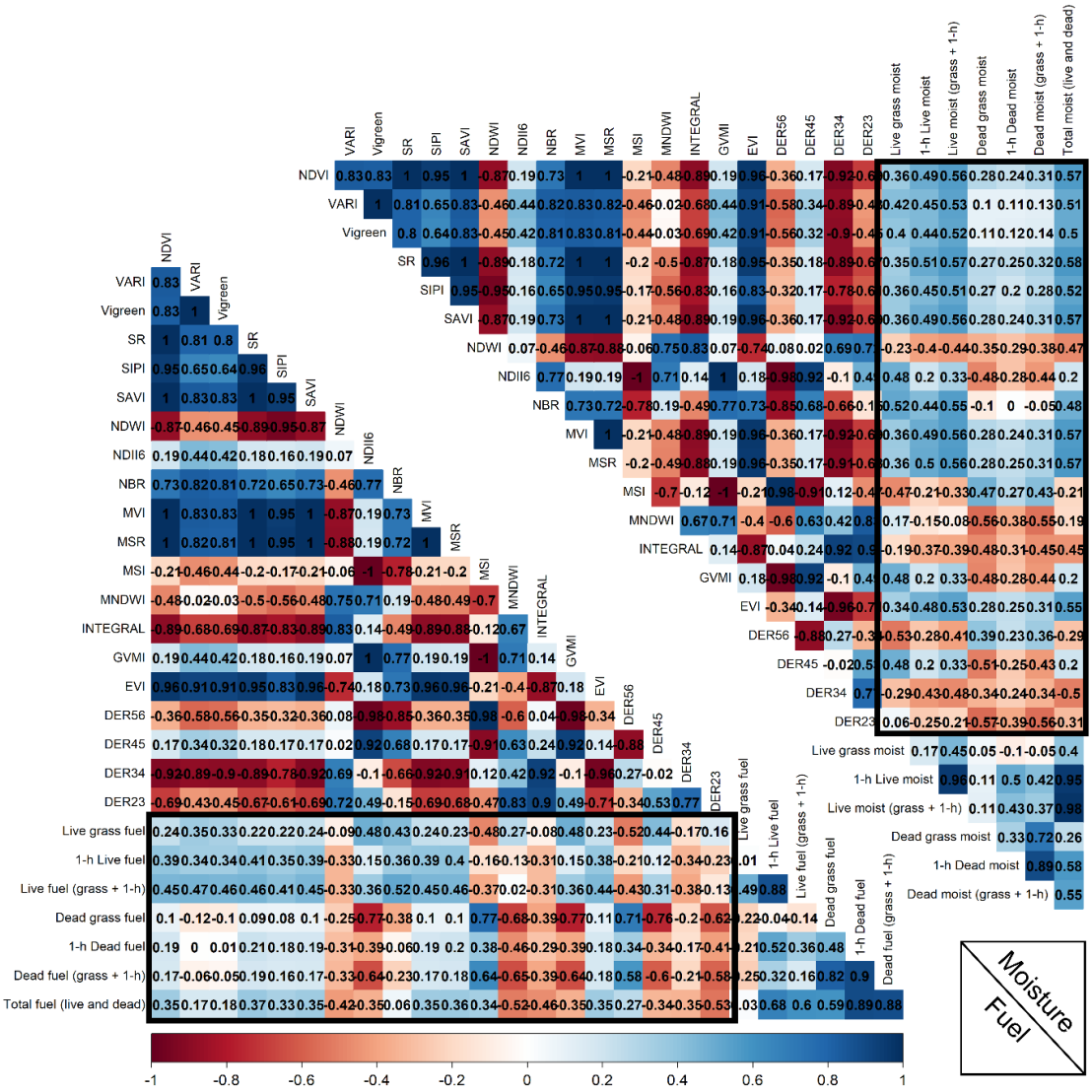

Figure 5. Correlations between moisture content and fuel load for different classes and calculated vegetation indices

Figura 5. Correlações entre a umidade e carga de combustível em suas diferentes classes e os índices de vegetação calculados

The least expressive relationships between the humidity variables and VIs were between the moisture content of 1-h downed wood debris, and the correlations with the VARI, VIgreen, SIPI, SAVI, NBR, and DER56 indices were not statistically significant ($p < 0.05$) (Figure 5).

DISCUSSION

The correlations showed better performance among the dead fuel variables, especially for the load and moisture content of dead grass fuel and 1-h downed wood debris (<0.64 cm in diameter) vs. the variables extracted from satellite images. One possible reason for this behavior is that the sampling was conducted during the dry season and that fine (1-h time lag) and dry fuels were predominant in the Cerrado grassland areas.

Among the correlations obtained between the fraction values from SMA and the loads of the different fuel classes, the most expressive correlation was between dead grass fuel and SF ($r = -0.81$ for load and $r = -0.60$ for moisture content), demonstrating considerable influence of the presence of exposed soil in the relationship with the load and moisture content of grass fuel. When the correlation of the NPV fraction with the load and moisture content of dead grass fuel was evaluated, the result was $r = 0.75$ and $r = 0.55$ ($p < 0.01$) for load and moisture content, respectively. The relationships between the fraction values from SMA and fuel load variables differed

from those reported by Franke *et al.* (2018), who showed superior relationships between the NPV fraction variables whereas SF presented a weaker relationship.

The reflectance of the near-infrared band of the OLI sensor (NIR; 0.85–0.87 µm) showed a more significant relationship with the load variables and with the moisture content of the dead grass fuel and total fine dead fuel (grass + 1- h downed wood debris). Considering that the class comprised physiologically inactive vegetation or low moisture content, it showed an inverse relationship with near-infrared reflectance. As highlighted by Danson and Bowyer (2004), a significant inverse relationship exists between individual wavelengths and leaf water content. Working with data from the Multispectral Scanner System (MSS) sensor of Landsat and correlating with phytomass of green herbaceous vegetation, Merrill *et al.* (1993) found better correlations with the green band (0.5–0.6 µm; r = -0.64), while Zhang *et al.* (2018) showed stronger correlations between biomass and the green and red bands using Landsat data (TM and OLI sensors). Hadi *et al.* (2016) observed stronger correlations between canopy cover and mid-infrared reflectance (r = -0.78), showing no correlations with the near-infrared region.

Among the correlations between the VIs tested and fuel load variables, those that stood out involved NDII6, MSI, and GVMI. Analyzing the spectral bands and the indices used in the formulas, it can be observed that both present the near-infrared (NIR; 0.85–0.87 µm) and mid-infrared (SWIR1; 1.56–1.65 µm) bands, demonstrating the importance of the infrared regions for estimating fuel load in the present study. Near-infrared and mid-infrared regions have been used to estimate vegetation characteristics with several configurations (e.g., CHUVIECO *et al.*, 2002). According to Chuvieco *et al.* (2002), significant relationships between fuel moisture characteristics and mid-infrared regions may be based on the high absorption peaks in this spectral region. Li *et al.* (2022) used high-resolution images and machine learning techniques to estimate the biomass in West Texas pastures. They demonstrated that VIs, especially the NDVI using NIR, are effective in quantifying biomass, which is essential for fuel management in pasture areas. In the near-infrared region (0.72–1.1 µm), reflectance is almost constant and water absorption is generally low, while in the mid-infrared region (1.1–3.2 µm), water content considerably absorbs incident radiation (PONZONI; SHIMABUKURO; KUPLICH, 2012).

Using aboveground biomass estimate, Gao *et al.* (2020) found stronger correlations with NDVI with r = 0.62. Merrill *et al.* (1993) found correlations with r = 0.57 for the phytomass of living grassland vegetation vs. the vegetation index calculated using the ratio between the near-infrared bands and the green band. Considering the relationship between moisture content and VIs, Danson and Bowyer (2004) found stronger correlations with r = 0.78 and r = 0.58 for the water index (WI) and NDWI indices, respectively. Using linear regression modeling to estimate the moisture content of dead fuel with NDVI, Zormpas *et al.* (2017) obtained weak, non-significant correlations with r = 0.01. In the present study, the relationship between NDVI and fuel moisture content was positive and stronger for the live fuel classes (r = 0.36–0.56). García *et al.* (2020) obtained significant positive correlations between NDVI and live fuel moisture content, ranging from r = 0.22 to r = 0.87 ($p < 0.001$). Chuvieco *et al.* (2002) obtained more significant relationships between the Integral and Wetness indices with grass moisture content, with a value of r = 0.91 ($p < 0.01$). Among the correlations between grass moisture content and band reflectance, they obtained higher values of r = 0.88 with the mid-infrared bands (SWIR: 1.4–2.5 µm).

In this study, the relationships between live fuel variables (live grass, live shrub fuel, and total fine live fuel) and the independent variables were weaker than those of the dependent variables of dead fuels (dead grass; 1-h downed wood debris, and total fine dead fuel). However, using VIs contributed to improving the relationships with live fuels, demonstrating the importance of VIs in estimating live surface fuels. Costa-Saura *et al.* (2021) worked with an empirical model to estimate live fuel moisture content in areas of mixed vegetation using Sentinel-2 data and meteorological variables, demonstrating that indices such as NDMI are promising for the efficient monitoring of live fuels in areas of dense vegetation.

Among the spectral bands of the OLI sensor, the one that presented the strongest relationship with the live fuel classes was the mid-infrared region (SWIR1; 1.56–1.65 µm), followed by the red region (0.63–0.67 µm). Of the live fuel classes, only the mid-infrared region (SWIR1; 1.56–1.65 µm) did not present significant relationships with the live grass fuel class. A possible explanation for this behavior may be that the live grass fuel class was less predominant during the dry season and mixed with the dry grassland vegetation that was predominant during this period. The stronger relationship with the 1-h downed wood debris may be due to the higher moisture content of this type of material associated with the more significant load and its greater ease of distinction from herbaceous plants, which may have contributed to the stronger spectral relationship.

Regarding the effect of spectral resolution, Marino *et al.* (2020) used Sentinel-2 and MODIS data to estimate fuel moisture content in Mediterranean vegetation areas and demonstrated that spectral resolution influences the accuracy of estimates, with variable results depending on the combination of the spectral bands used. The moisture content is closely linked to the level of absorption of electromagnetic radiation in the mid-infrared region, that is, the higher the moisture content of the material, the greater the absorption of radiation and, consequently, the lower the reflectance (CHUVIECO *et al.*, 2002; PONZONI; SHIMABUKURO; KUPLICH, 2012).

CONCLUSIONS

The fractions of NPV, GV, and SF obtained by SMA showed significant and more expressive relationships with dead fuel load and total fine fuel load (live and dead; <0.64 cm diameter). SF showed stronger correlations than the other fractions, demonstrating considerable influence of exposed soil with regard to determining the fuel load from satellite images in the Cerrado grassland phytophysiognomy.

The reflectance variables obtained from the Landsat 8 OLI satellite images and the calculated VIs showed the strongest relationships with dead fuel classes. The best relationships were found for the reflectance of the near-infrared (NIR) band among the Landsat 8 OLI bands, and the VIs that stood out included near-infrared (NIR) and mid-infrared (SWIR1) regions in their formulations.

ACKNOWLEDGMENTS

The authors acknowledge the National Council for Scientific and Technological Development (CNPQ) for the financial support granted to carry out this research, and the Serra Geral do Tocantins Ecological Station managers, Ana Carolina Sena Barradas, Marco Assis Borges, and Máximo Menezes Costa, for their support in the planning and logistics of the field investigation.

REFERENCES

CHRYSAFIS, I.; MALLINIS, G.; GITAS, I.; TSAKIRI-STRATI, M. Estimating Mediterranean forest parameters using multi seasonal Landsat 8 OLI imagery and an ensemble learning method. **Remote Sensing of Environment**, [S. l.], v. 199, p. 154–166, 2017. DOI: 10.1016/J.RSE.2017.07.018.

CHUVIECO, E.; RIAÑO, D.; AGUADO, I.; COCERO, D. Estimation of fuel moisture content from multitemporal analysis of Landsat Thematic Mapper reflectance data: Applications in fire danger assessment. **International Journal of Remote Sensing**, [S. l.], v. 23, n. 11, p. 2145–2162, 2002. DOI: 10.1080/01431160110069818.

COSTA-SAURA, J.M.; BALAGUER-BESER, A.; RUIZ, L.A.; PARDO-PASCUAL, J.E.; SORIANO-SANCHO, J.L. Empirical models for spatio-temporal live fuel moisture content estimation in mixed mediterranean vegetation areas using sentinel-2 indices and meteorological data. **Remote Sensing**, [S. l.], v. 13, n. 18, p. 3726, 2021. DOI: 10.3390/rs13183726.

DANSON, F. M.; BOWYER, P. Estimating live fuel moisture content from remotely sensed reflectance. **Remote Sensing of Environment**, [S. l.], v. 92, n. 3, p. 309–321, 2004. DOI: 10.1016/J.RSE.2004.03.017.

FORBES, B.; REILLY, S.; CLARK, M.; FERRELL, R.; KELLY, A.; KRAUSE, P.; MATLEY, C.; O'NEIL, M.; VILLASENOR, M.; DISNEY, M.; WILKES, P.; BENTLEY, L.P. Comparing Remote Sensing and Field-Based Approaches to Estimate Ladder Fuels and Predict Wildfire Burn Severity. **Frontiers in Forests and Global Change**, [S. l.], v. 5, p. 818713, 2022. DOI: 10.3389/ffgc.2022.818713.

FRANKE, J.; BARRADAS, A.C.S.; BORGES, M.A.; MENEZES COSTA, M.; DIAS, P.A.; HOFFMANN, A.A.; OROZCO FILHO, J.C.; MELCHIORI, A.E.; SIEGERT, F. Fuel load mapping in the Brazilian Cerrado in support of integrated fire management. **Remote Sensing of Environment**, [S. l.], v. 217, p. 221–232, 2018. DOI: 10.1016/J.RSE.2018.08.018.

GALE, M. G.; CARY, G. J.; VAN DIJK, A. I. J. M.; YEBRA, M. Forest fire fuel through the lens of remote sensing: Review of approaches, challenges and future directions in the remote sensing of biotic determinants of fire behaviour. **Remote Sensing of Environment**, v. 255, p. 112282, 2021. DOI: 10.1016/j.rse.2020.112282.

GAO, X.; DONG, S.; LI, S.; XU, Y.; LIU, S.; ZHAO, H.; YEOMANS, J.; LI, Y.; SHEN, H.; WU, S.; ZHI, Y. Using the random forest model and validated MODIS with the field spectrometer measurement promote the accuracy of estimating aboveground biomass and coverage of alpine grasslands on the Qinghai-Tibetan Plateau. **Ecological Indicators**, [S. l.], v. 112, p. 106114, 2020. DOI: 10.1016/J.ECOLIND.2020.106114.

GARCÍA, M.; RIAÑO, D.; YEBRA, M.; SALAS, J.; CARDIL, A.; MONEDERO, S.; RAMIREZ, J.; MARTÍN, M.P.; VILAR, L.; GAJARDO, J. A.; USTIN, S. Live Fuel Moisture Content Product from Landsat TM Satellite Time Series for Implementation in Fire Behavior Models. **Remote Sensing**, [S. l.], v. 12, n. 11, p. 1714, 2020. DOI: 10.3390/RS12111714.

GORELICK, N.; HANCHER, M.; DIXON, M.; ILYUSHCHENKO, S.; THAU, D.; MOORE, R. Google Earth Engine: Planetary-scale geospatial analysis for everyone. **Remote Sensing of Environment**, [S. l.], v. 202, p. 18–27, 2017. DOI: 10.1016/J.RSE.2017.06.031.

HADI; KORHONEN, L.; HOVI, A.; RÖNNHOLM, P.; RAUTIAINEN, M. The accuracy of large-area forest canopy cover estimation using Landsat in boreal region. **International Journal of Applied Earth Observation and Geoinformation**, [S. l.], v. 53, p. 118–127, 2016. DOI: 10.1016/J.JAG.2016.08.009.

ICMBIO. **Management plan for Serra Geral do Tocantins Ecological Station** [Plano de manejo para Estação Ecológica Serra Geral do Tocantins (EESGT)]. 1. ed. Brasília. v. 1. 2014.

KENNEDY, M.C.; PRICHARD, S.J.; MCKENZIE, D.; FRENCH, N.H.F. Quantifying how sources of uncertainty in combustible biomass propagate to prediction of wildland fire emissions. **International Journal of Wildland Fire**, [S. l.], v. 29, n. 9, p. 793–806, 2020. DOI: 10.1071/WF19160.

LECINA-DIAZ, J.; MARTÍNEZ-VILALTA, J.; ALVAREZ, A.; VAYREDA, J.; RETANA, J. Assessing the Risk of Losing Forest Ecosystem Services Due to Wildfires. **Ecosystems**, [S. l.], v. 24, n. 7, p. 1687–1701, 2021. DOI: 10.1007/s10021-021-00611-1.

LI, Z.; ANGERER, J.P.; JAIME, X.; YANG, C.; WU, X.B. Estimating Rangeland Fine Fuel Biomass in Western Texas Using High-Resolution Aerial Imagery and Machine Learning. **Remote Sensing**, [S. l.], v. 14, n. 17, p. 4360, 2022. DOI: 10.3390/RS14174360.

MARINO, E.; YEBRA, M.; GUILLÉN-CLIMENT, M.; ALGEET, N.; TOMÉ, J.L.; MADRIGAL, J.; GUIJARRO, M.; HERNANDO, C. Investigating Live Fuel Moisture Content Estimation in Fire-Prone Shrubland from Remote Sensing Using Empirical Modelling and RTM Simulations. **Remote Sensing**, v. 12, n. 14, p. 2251, 2020. DOI: 10.3390/RS12142251.

MERRILL, E.H.; BRAMBLE-BRODAHL, M.K.; MARRS, R.W.; BOYCE, M.S. Estimation of green herbaceous phytomass from Landsat MSS data in Yellowstone National Park. **Journal of Range Management**, [S. l.], v. 46, n. 2, p. 151–157, 1993. DOI: 10.2307/4002273.

PONZONI, F.J.; SHIMABUKURO, Y.E.; KUPLICH, T.M. **Sensoriamento remoto da vegetação**. 2. ed. [s.l.] : Oficina de Textos, 2012. v. 1

RIBEIRO, J.F.; WALTER, B.M.T. **As principais fitofisionomias do Bioma Cerrado**. In: Cerrado: ecologia e flora. 1. ed. Brasília-DF: Embrapa Cerrados, 2008. v. 1p. 152–212.

ROTHERMEL, R.C. **A mathematical model for predicting fire spread in wildland fuels**. Forest Service - Rocky Mountain Research Station, Usda, [S. l.], n. Research Paper INT-115, p. 1–48, 1972.

SHARMA, S.; DHAKAL, K. Boots on the Ground and Eyes in the Sky: A Perspective on Estimating Fire Danger from Soil Moisture Content. **Fire**, [S. l.], v. 4, n. 3, p. 45, 2021. DOI: 10.3390/fire4030045.

SCHROEDER, M.; BUCK, C. **Fire Weather:** A Guide for Application of Meteorological Information to Forest Fire Control Operations. USDA Forest Service, Agriculture Handbook 360, [S. l.], 1970.

VERMOTE, E.; ROGER, J. C.; FRANCH, B.; SKAKUN, S. LASRC (Land Surface Reflectance Code): Overview, application and validation using MODIS, VIIRS, LANDSAT and Sentinel 2 data's. **International Geoscience and Remote Sensing Symposium (IGARSS)**, [S. l.], v. 2018- July, p. 8173–8176, 2018. DOI: 10.1109/IGARSS.2018.8517622.

YEBRA, M.; QUAN, X.; RIAÑO, D.; ROZAS LARRAONDO, P.; VAN DIJK, A.I.J.M.; CARY, G.J. A fuel moisture content and flammability monitoring methodology for continental Australia based on optical remote sensing. **Remote Sensing of Environment**, [S. l.], v. 212, p. 260–272, 2018. DOI: 10.1016/J.RSE.2018.04.053.

ZHANG, C.; DENKA, S.; COOPER, H.; MISHRA, D.R. Quantification of sawgrass marsh aboveground biomass in the coastal Everglades using object-based ensemble analysis and Landsat data. **Remote Sensing of Environment**, [S. l.], v. 204, p. 366–379, 2018. DOI: 10.1016/J.RSE.2017.10.018.

ZORMPAS, K.; VASILAKOS, C.; ATHANASIS, N.; SOULAKELLIS, N.; KALABOKIDIS, K. Dead fuel moisture content estimation using remote sensing. **European Journal of Geography**, [S. l.], v. 8, n. 5, p. 17–32, 2017.